A0- Characterization of the *Picosecond Pulsed Fiber Laser*

Courtney Clarke

School of Engineering and Applied Science

Miami University

Oxford, OH 45056

Jinhao Ruan and James Santucci

A0PI

Accelerator Division

Fermilab National Accelerator Laboratory

Batavia, IL 60510

Summer Internship in Science and Technology (SISTP) Program

Date: August 3rd, 2010

Abstract: The *Picosecond Pulsed Fiber Laser* (PSL) laser will act as the *new seed laser* in the New Muon Lab Test Area at Fermilab National Accelerator Laboratory. The Nd:YLF laser currently running in A0 laboratory is the model which the PSL is based on. The PSL will produce a train of pulses at 81.25 MHz with a wavelength of 1054 nm and a pulse width of 5 ps. The stability of the seed laser is crucial to the success of A0 Photoinjector's mission, which is to provide stable electron bunches for research and diagnostics. With a phase lock loop directly operating at a 1.3 GHz clock, the new PSL system is more suitable for this application. In order to directly compare the PSL to the current A0 seed laser system the laser is being characterized for the duration of the summer program. The results of these tests concluded that the laser exhibits significant power drift with time. This drift is attributed to the shifting of the modulator bias component in the laser. A proposed solution for this issue is a feedback circuit that will adjust the modulator voltage for optimal power and mode locking. This modulator bias difficulty will be further looked at succeeding the completion of the summer session.

Table of Contents

Introduction:

- **Fermi National Accelerator Laboratory**

My project was conducted under the Summer Internship in Science and Technology (SIST) program. The SIST program within Fermilab targets undergraduates in science and technology, providing students with summer projects that are a part of the regular laboratory research taking place at Fermilab. There are many programs like SIST, TARGET, GEM, and FaST that are results of cooperative relations between Fermilab and other organizations like the Department of Energy (DOE), Northern Illinois University, and the National Science Foundation (NSF) that provides students with research opportunities. In addition to being responsible for Fermilab, DOE manages and funds a large part of the high energy research in the United States.

The Office of Science, in DOE's high energy support division focuses mainly on the advancement and development of important cutting-edge technologies, and training youth for the future of scientific research [1]. The Office of Science supports more than 7,000 research projects at universities, in the U.S. industry, in the non-profit sector and in national laboratories like Fermilab [2].

The current and future role of Fermilab, in DOE's plans, is to advance the understanding of the fundamental nature of matter and energy. Fermilab's facility is open for user research where people from around the world can perform experiments using Fermilab's technology and resources, especially its protons, electrons, and neutrinos. As a leading accelerator laboratory, Fermilab has several major accelerators including the *Linear accelerator (LINAC),* the *Booster,* the *Main injector,* and the *Tevatron* all used to produce an early universe environment to solve the mysteries of the cosmos and to develop the S*tandard Model* of an atom.

Fermilab is also known for its superconducting magnet research. The electromagnets that are the main component of MRI scanners, were originally developed for the Tevatron. Great importance falls on Fermilab's current research on superconducting radio-frequency (SCRF) cavities. These cavities have the potential for nuclear waste treatment and are the main component in the acceleration of protons and electrons for examination [3].

- **A0 Experiment and the NML injector:**

The A0 photoinjector (A0PI), the Accelerator division's A0 Lab is a research and development group whose predominant concern is the functionality of the photoinjector for user research. The goal of the project is to produce and maintain an "*18 MeV electron linac that produces a high-intensity, low emittance beam*[4]" for high energy particle research. This work is done in

collaboration with DESY (Deutsches Elektronen-Synchrotron) in Hamburg and Zeuthen Germany[5], and Northern Illinois University.

A0PI relies on many sequential processes for functionality. Parts of A0PI include a drive laser, the electron RF-gun, radio frequency (RF) accelerating cavities, and the electron beamline. The seed laser for the A0PI drive laser creates a 1 MHz collection of 5 ps pulses at 1054 nm wavelength. The pulses produced at this section of the drive laser are from a phase-stabilized, mode-locked Nd-doped Yttrium Lithium Fluoride (Nd:YLF) oscillator and a fast selection Pockel cell, which can also be modeled as a *pulse selector*. The pulse selector chooses a small cluster of pulses to proceed beyond the drive laser to the RF-gun and the rest are analyzed for anomalies. These select pulses are amplified twice, once through a *multipass amplifier* which amplifies x1000, and then again through a *twopass amplifier* which amplifies x40. The pulses then advance through two doubling crystals to induce the fourth harmonic wavelength from 1054 nm (infrared), to 527 nm (green), and lastly to 263 nm which is in the ultraviolet (UV) range. Optical media direct the UV beam through a beam pipe to the photocathode in the RF-Electron gun.

To produce the *photoelectric effect* the photocathode is bombarded with the UV pulses. A photocathode is a cathode that emits electrons by means of the *photoelectric effect*. Surface electrons attain their energy from short wavelength UV pulses. The energy absorbed is the defined amount of energy for the electron to be ejected from the surface of the photocathode. The ultra-short, 3 ps (σ), UV laser pulses hit a target producing unpolarized electron bunches of about the same length, which are manipulated and steered using electromagnets, and accelerated with SCRF cavities. These electrons are open to other research facilities for experimentation and research.

- **Project:**

The New Muon Lab (NML) Photoinjector is based on A0PI technology. The seed laser under study is an upgrade of the Nd:YLF crystal to a Ytterbium Doped Fiber Amplified (YDFA) Picosecond Pulsed Fiber Laser (PSL). The objective of this project is to perform the necessary comparative tests to contrast the stability of the PSL system with respect to the Nd:YLF.

The PSL is predicted to produce a more stable, less *jittery* train of pulses. In addition, the PSL is more acclimated and can employ different settings to manipulate the pulses possibly obtaining a higher electron efficiency and quality. The unit is more robust with a life time of 50,000 hours. This comes out to be about a lifetime 10 times longer than the Nd:YLF, and replacement of the diode is less problematic. Other advantages of this laser include its ability to be precisely and directly locked to 1.3 GHz. The Nd:YLF is locked only to a harmonic of 1.3 GHz at 81.25 MHz. 1.3 GHz is the frequency at which the SCRF cavities perform optimally due to engineering.

Some disadvantages that arise from handling new technology is unfamiliarity. The fiber laser has not been used in A0PI and is considered neoteric technology. It is still under rigorous research and experimentation at facilities like DESY (Please refer to [8]). The characterization of the PSL is crucial for its use in the NML test area. Primary areas of focus include phase stability, wavelength, jitter and power. Setup and operation advice will also be touched upon.

- **Background:**
    - **A0 Experimental technology for NML**

Currently the A0PI is in the process of preparing for the future relocation to the NML Facility. NML is a SCRF accelerator test facility under construction at Fermilab. The accelerator will consist of a photocathode, an RF-electron gun, a Photoinjector, a beam acceleration section of up to 6 TESLA Test Facility (TTF)-type (a.k.a. ILC-type) cryomodules, multiple downstream beamlines for testing diagnostics and conducting beam tests, and a high power beam dump. Upon completion, the facility will be capable of generating a 1.5 GeV electron beam. Other important uses of this facility include the testing of accelerator components, the testing of RF power equipment and instrumentation, and the development of low level radio frequency (LLRF) and control system for future SCRF accelerators such as the International Linear Collider (ILC) and the Project-X linear proton accelerator.

To make the transition to NML, the PSL will be required to perform the fundamental tasks of the A0PI laser. To recap, these roles include the use of an 81.25 MHz oscillator for a diode pumped (currently from the Nd:YLF) seed laser at 1054 nm wavelength pulsed at 5 ps producing an 81.25 MHz pulse train. Once the move is completed it is anticipated that the NML-PI beamline will be functional in less than year. The PSL seed laser system currently under investigation for the NML test area was produced by Eureka. Recently purchased from Calmar laser, the PSL is a new line of fiber-based technology that surpasses barriers in laser stability. The doping of the laser fibers has allowed for higher potential in laser amplification along with lower jitter. The most popular dopants for pulse fiber laser technology are the Erbium and the Ytterbium dopants. The fiber lasers are more stable than flash-lamp lasers, and incur less noise travelling over space. This is crucial when running a cycle that produces “identical” electron bunches.

- **Laser technology**

Some fundamental concepts of laser technology will be explained in this section. Light is a form of an electromagnetic wave. These waves can be defined by their wavelength, which also determines the color of the light emitted. The wavelength is the spacing of one independent cycle in the wave. Waves are said to be in phase if their peaks align and their crests align regardless of the propagation through time and space. The difference between normal light and laser light is that normal light can have several wavelengths simultaneously which are randomly directional and phased. This light is emitted from light bulbs and other common light products. On the other hand, a laser emits coherent light with one or a definite amount of wavelengths that are in phase.

Furthermore, laser light propagates over a narrow cross sectional area, and hence is unidirectional.

Wavelengths of the light fall into 7 main categories or colors, but we are only interested in 3: infrared or IR (700 nm to 1 mm), visible (400-700 nm), and ultraviolet or UV (180-499 nm).

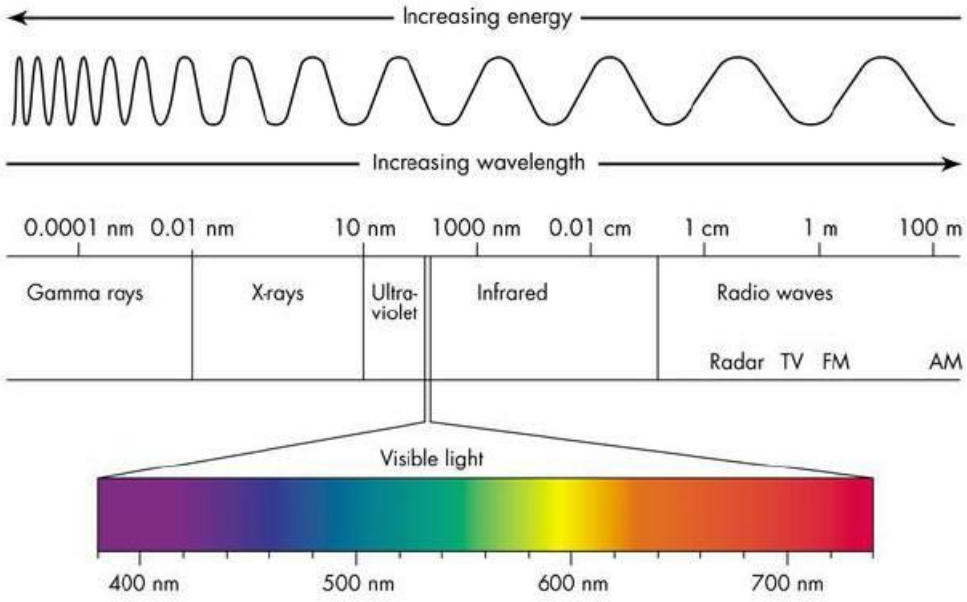

Figure (1): The electromagnetic spectrum. [6]

The wavelength also corresponds to different energies of the travelling photon. They correlate according to the following equation:

$$f = \frac{c}{\lambda} \qquad \text{Equation [1]}$$

f is the frequency of the photon, c is the speed of light in vacuum, and λ is the wavelength. This equation and the *Planck- Einstein* equation can be used the find the energy of a photon with a specific wavelength according to:

$$E = \frac{hc}{\lambda} \qquad \text{Equation [2]}$$

Where E is energy and $h = 6.626068 \times 10^{-34}$ J/s (Planck's constant).

The laser uses 3 parts to produce coherent light via stimulated emission, hence the acronym laser or light amplification by stimulated emission of radiation. Stimulated emission occurs when an excited electron is disturbed by a passing photon and that electron releases another coherent photon. The laser parts include the excitation mechanism, the excitation medium, and the optical resonator (cavity).

The excitation mechanism is the initial source of energy or light. It can be electricity, flash lamps, or in our case another laser. The PSL uses a laser diode as an excitation mechanism.

The next part is the lasing medium. The medium produces coherent light after being excited by the excitation mechanism. In our case we use a Ytterbium doped fiber. At this stage the light is emitted in random directions.

The last part of the laser is the optical resonator or cavity. Here the random light is reflected between a fully reflective and semi-transparent mirror for amplification. When the light obtains a specific intensity it can pass through the partially reflected end of the cavity as the laser light.

From the functional diagram of the PSL, the lasing medium is also referred to as a Ytterbium (Yb) Doped Fiber amplifier (YDFA).

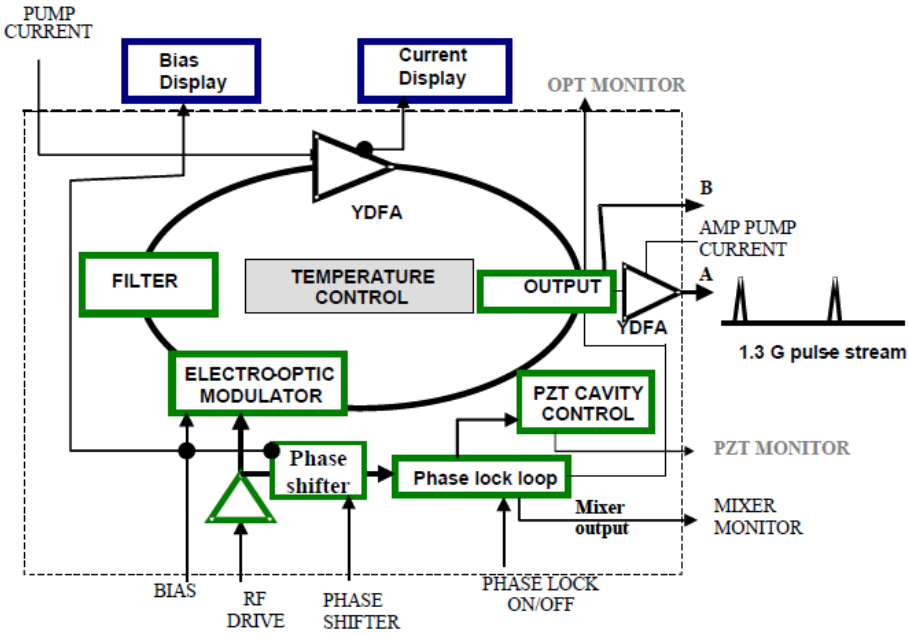

Figure (2): Diagram of System [7]

The amplifier controls the pump current reaching the Yb-doped fiber thus controlling the optical gain. This is the labeled YDFA within the ellipse in the above figure. As denoted in the diagram the light comes out as a 1.3 GHz pulse stream, as required.

- **Fiber Lasers**
  - **About**
    - **Solitary Wave Equation**

A very good text on fiber lasers is called "*Fiber Laser Master Oscillators for Optical Synchronization systems"* by Axel Winter [8]. He explains the processes of a fiber laser, and mathematically depicts how they work. He uses Maxwell's equation deriving a wave equation for isolating polarizable nonmagnetic materials:

$$\nabla^2 E - \frac{1}{c^2}\frac{\partial^2 E}{\partial t^2} = \frac{\mu_0 \partial^2 P}{\partial t^2} \qquad \text{Equation [3]}$$

Making a few assumptions including an immediate polarization response, a negligible non-linearity (when the superposition principle is no longer valid) in polarization density *P*, and the sufficiency of the scalar approach assuming the optical fields remain constant for the length of the fiber the nonlinear Schrödinger equation can be derived:

$$\frac{\partial A}{\partial z} + \frac{i\beta_2}{2}\frac{\partial^2 A}{\partial T^2} + \frac{\alpha}{2}A = i\gamma|A|^2 A \; where \; T = t = \frac{z}{v_g} \equiv t - \beta_1 z \qquad \text{Equation [4]}$$

Where A is a plane wave, β_2 is chromatic dispersion or broadening in time, γ is fiber non-linearities and α is the fiber losses. These variables account for how an optical signal responds while it travels through fiber in time and space. The signal at each component of the fiber travels at varying speeds due to these non-linear effects and losses. However, the fiber can only sustain a narrow bandwidth of wavelengths centered at a main wavelength. The different wavelengths travel at different speeds along the fiber [9].

From the nonlinear Schrodinger equation the solitary wave equation can be derived:

$$\frac{\partial A}{\partial z} = i\gamma|A|^2 A - \frac{i\beta_2}{2}\frac{\partial^2 A}{\partial T^2} \; with \; \gamma = \frac{n_2 \omega_0}{c S_{eff}} \qquad \text{Equation [5]}$$

S_{eff} is the effective area of the fiber, n_2 is the refractive index, $\omega_0$is the definite frequency and v_g is the moving group velocity. This equation assumes no fiber losses, which simplifies analysis. It noted that the majority of the nonlinearities in the gain fiber can be accounted for with pulse energy and the pulse duration. The solitary wave equation more simply states that if A represents the nonlinearities that are dependent on pulse duration and pulse energy and are always present in the fiber regardless of the fiber properties, and β_2 represents nonlinearities produced from only the pulse duration, then it is possible to create a combination of pulse duration and pulse energy that will allow $\frac{\partial A}{\partial z} = 0$. As a result the nonlinearity and the fiber losses can be disregarded, because they cancel out [8].

- Mode Locking

Winter also as explains the process of active and passive *mode-locking*. Mode-locking is the only method available to achieve the ultra-short (in our case approximately 5 ps) pulses. Winter

proposes two main types of mode locking, but the method of interest is active amplitude modulation (AM) mode locking, which is the method that the PSL uses.

The method by which the PSL mode-locks requires the use of plane waves to analogize, because in actuality laser light acts more like a traveling wave. First, laser pulses are created by "*the superposition of plane wave of different wavelengths* [in the optical cavity] [8]." A laser cavity can be made in such a way that the laser can oscillate at only one frequency, so the standing waves or *longitudinal modes* constructively interfere at only that frequency and are completely destructive at other frequencies [10]. A longitudinal mode is a standing wave that is a multiple of the fundamental frequency. It is longitudinal because it propagates along the cavity. This is why a laser cavity is selective of which frequencies it can support, because all others will cancel out. Winter uses the analogy that "*the superposition of N modes* [in a cavity] *is similar to the interference of N planar waves* [8]." This is attained by adjusting the length of the cavity to allow for this maximum interference if the condition below holds true:

$$n\lambda_n = 2L \qquad \text{Equation [6]}$$

Where λ_n is the wavelength of the longitudinal mode n and L is the length of the cavity. If this condition is followed, then the modes will interfere to create pulses. To keep this condition true, the cavity length is adjusted, in our case using a piezoelectric stage. The superposition of these modes in a cavity generates periodic intensity maxima due to their interference. However, since the modes are independent of each other, the phases have a tendency to drift with time causing random flashes rather than periodic pulses. Therefore, in addition to this condition, the modes must remain phase locked with respect to each other. This is accomplished with amplitude modulation. By modulating the cavity with the frequency difference of the adjacent modes [8], the phases are locked. The mode spacing is determined by the cavity. The interference pattern that produces periodic pulses is called mode-locking, and it is what is relied on to created pulses at a specific repetition rate.

Active mode locking uses an active element to modulate the amplitude. The amplitude is modulated with a frequency equal to or a harmonic of the mode spacing. In our case, the amplitude is modulated with a 1.3 GHz RF-signal as decided by the cavity.

With the PSL system, the active mode locking element is produced and maintained by an *electro-optics modulator*, and a *PZT cavity control*. The PZT cavity control controls the cavity length for stable mode-locking, and controls the frequency of the pulse train maintaining it at 1.3 GHz. The mode-locking is adjusted by the modulator which is manually controlled using the modulator bias voltage, adjustable by a knob on the front panel [7]. Issues arose with the modulator bias voltage and the output power of the laser, which will be discussed later in the report.

- **Electro-optic Modulator & Modulator Bias control**

As referred to in the mode-locking section, a method of keeping mode-lock is amplitude modulation. This can be achieved by manipulating the refractive index of the fiber the signal travels through, thus manipulating the phase. The refractive index defines how fast light travels through a media, and is determined by that media. As explained above the laser pulses are amplitude modulated. The mode of modulation is the *Lithium Niobate (LN) modulator*. This device can be used to modulate the amplitude or intensity (AM), or the phase (FM) is a given signal.

The way the LN modulator causes mode locking is by forcing the modes to phase lock. An analogy that describes the method of modulation is the opening and closing of the blinds of a window to let light in or block it out. It acts as an attenuator of unwanted phases and a preserver of the correct phase. If the attenuator is constantly on, then the laser light will not be able to intensify by reflecting between the mirrors in the cavity. The laser would be smothered. If the attenuator is turned off at the wrong time, then the pulses produced by interference will also be blocked, but amplification will still occur, because some light passes through. The two possibilities is that can occur are that the light will be emitted in intensity spurts causing a random signal, or if left to intensify further, the light with be a continuous wave at the frequency of the cavity. These are not desired results for the periodic production of electrons. Therefore, the attenuator would have to be on precisely until the pulse approaches it, then the attenuator turns off exactly as the pulse passes through, and then turns on again. This will cut off any intensities due to drifting phases, preventing them from superimposing with the phased locked pulse leaving a “perfect” 1.3 GHz pulse train [10]. This is because in a cycle only the pulse at 1.3 GHz will remain unattenuated, and it will amplify at the normal rate while all the other pulses remain small.

The LN modulator, acting as the attenuator, keeps the unspecified pulses attenuated. The optical signal travels through the modulator via a phase-matching (PM) Fiber, and is split into two paths. If a voltage is applied to the RF electrode, creating an electric field across the split fiber, the signals are forced out of phase. When the voltage is turned off the signal recombines back together in phase.

While the voltage is on, the material which the signal travels through induces an electro-optic effect that puts the phase of one split fiber back and the other ahead. To do this, the refractive index of the material changes with the voltage as the signal passes through. While the voltage is on, when the signals come back together they are completely out of phase. These “on” and “off” are the two situations characterized as “0” and “1” in the figure below. When the signals are in phase they are allowed to pass through the modulator to create a pulse train. When they are out of phase, the signals interfere with each other so they cannot pass through the modulator. The voltage difference is what causes the two cases to occur, so a 1.3 GHz oscillating RF signal will induce the necessary voltage difference.

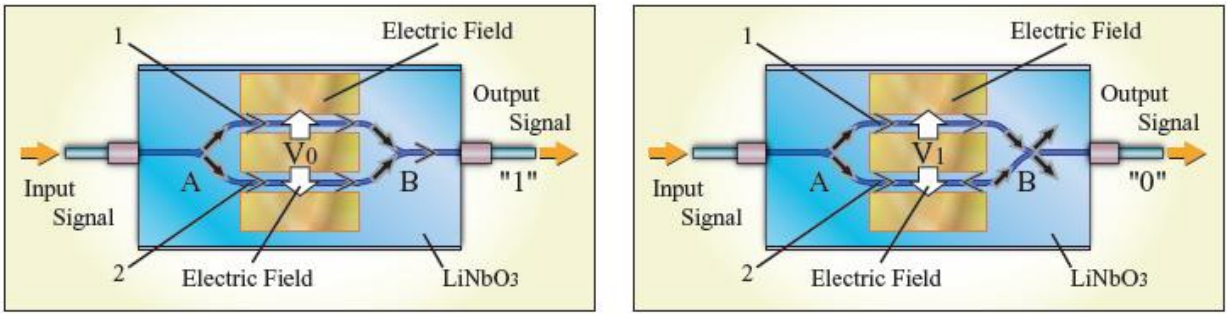

Figure (3): LN modulator [11]

The modulator bias voltage is what adjusts the modulator to its operational parameters. When travelling through the fiber, the voltage signal experiences "DC drift." This is when the voltage transmission curve shifts from what is known as *quadrature point*. This is the point where the modulator bias works best, and provides the finest mode-locking. By adjusting the modulator bias voltage, the transmission curve can be shifted back to quadrature for operation.

- **Gain Fiber**

Fiber lasers are a new field in research. Gain fibers are used to amplify the laser signal to an intensity that can be used for experimental purposes. Usually the elements used are rare-earths like Neodymium, Erbium and Ytterbium. The fiber used for the PSL is Ytterbium doped. The incident rays are amplified when passing through the fiber allowing for stimulated emission based on the wavelength of the light. The type of dopant determines what class the laser falls under. For example, a Yb laser uses a level 3 lasing scheme. Yb's simple atomic structure has one excited state manifold $^2F_{5/2}$ that can be reach by near infrared photons or visible light wavelengths from the ground state $^2F_{7/2}$.

The gain process occurs by pumping the fiber to population inversion, where there is "*a continuous number of available electrons for transition to a lower state emitting photons*[12]." For a Yb-doped fiber, pumping and amplification occurs in the transition between ground and excited manifolds. Population inversion occurs because the time in between excitation and relaxation is long enough for other electrons to excite. The fiber is pumped with photons of the right frequency and the electrons are stimulated to release other photons [13] (stimulated emission). The pumped photon and additional photon are not absorbed and are amplified in the cavity to be emitted as laser light once the intensity is enough to pass through the semi-transparent end of the cavity. In addition, the released photon is in phase with the pump photon for coherent laser light.

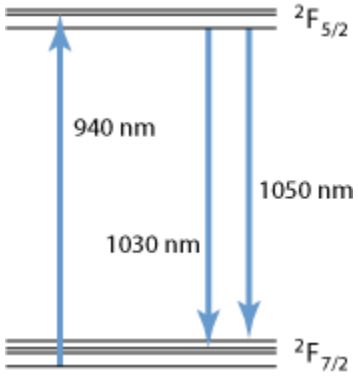

Figure (4): Atomic structure of Yb^{3+} ion from a Yb-YAG laser [14]

- **System:**
  - ***Picosecond Pulsed Fiber Laser (PSL)*:**

The laser needs to follow the scheme presently in A0. The output power emitted from the PSL should be about 100 mW, it should have a frequency of 1.3 GHz, a wavelength of 1054 nm, and a pulse length of 5 ps. The electronic pulse generator is to pick the pulses that are 81.25 MHz from the 1.3 GHz signal. This will cause the total power to drop 6-7 mW. The low dispersion amplifier will amplify the weak signal to about 400 mW or so allowing it to proceed through the beamline. This setup also allows for pulse selection variability, so that other frequency pulses can be used if necessary rather than the 81.25 MHz.

- ***Low Dispersion Amplifier* and *Electronic Pulse Generator***

The low dispersion amplifier is what will amplify the PSL to the equivalent of the signal outputted by the current laser. The weak signal is amplified about x10, and then will proceed to the *multi-pass* and *two-pass* amplifiers in the A0 laboratory. The low dispersion amplifier can produce a small signal gain of >30 dB, and the laser is emitted at a free space collimated beam[15].

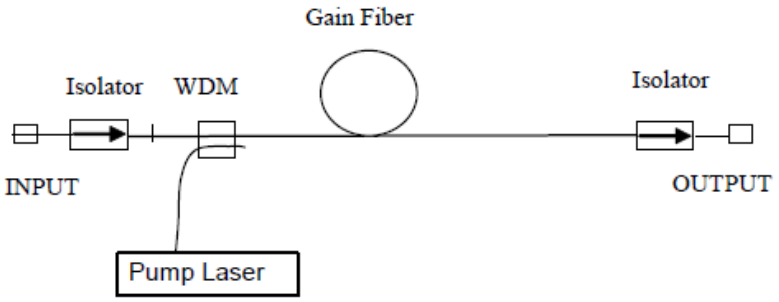

Figure (5): Scheme of low dispersion amplifier [15]

In addition, the electronic pulse generator allows for pulse selection. The pulse generator will select the 81.25 MHz pulses producing a more stable version of the beam currently in A0. The amplifier and pulse generator were not testable within the time constraints, so all tests were done strictly on the PSL. In the future, further tests will be needed to incorporate these devices.

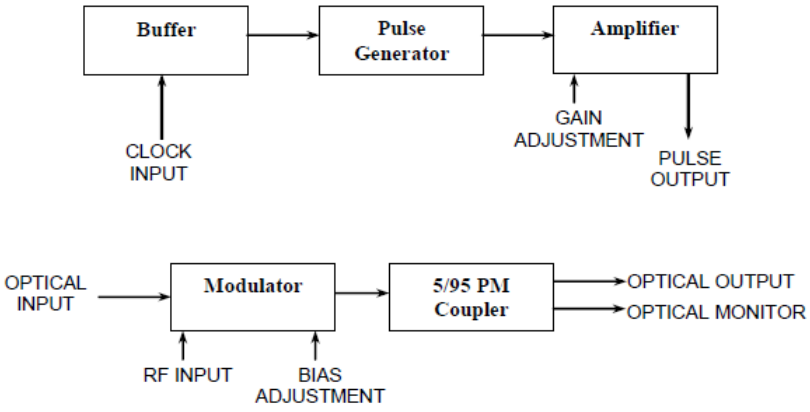

Figure (6): Scheme of functions block for electronic pulse generator [16]

Methods:

- **Instrumentation**
  - **System Schematic**

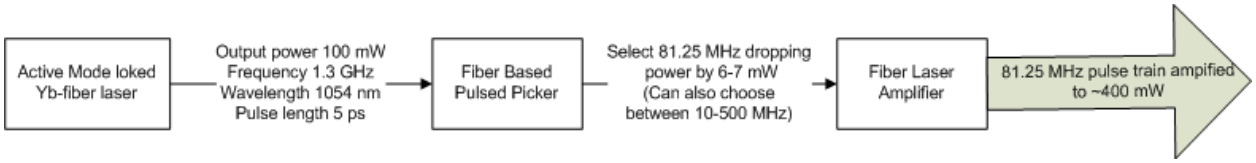

Figure (7): System Schematic for PSL including the *low dispersion amplifier*, and *electronic pulse generator*

  - **Pulse Width: *Autocorrelator***

One of the devices that will be used to characterize the PSL is an autocorrelator. The autocorrelator measures the pulse width. It is crucial that the pulse be picoseconds in length for the subsequent production of electrons at the required intervals. The current pulse width of the A0 laser is 5 ps.

The autocorrelator "*turns temporal information into spatial information* [17]." The pulse is split into two equivalent beams after passing through a beamsplitter and follows the path as denoted in figure (8). The temporal delays of the beams are detected with a photomultiplier and the time delay is related measuring the integrated signals with the following relation:

$$S(\tau) \sim \int_{-\infty}^{\infty} I_A \times I_B(t-\tau)dt \qquad \text{Equation [7]}$$

This is proportional to the second-order correlation function by:

$$G_2(\tau) = \int_{-\infty}^{\infty} \frac{I(t)I(t-\tau)dt}{\int_{-\infty}^{\infty} I^2(t)dt} \qquad \text{Equation [8]}$$

This autocorrelation function can be averaged over a large number of pulses, and is approximated with a Gaussian profile. The Gaussian's full-width-at-half-max is used to characterize the pulse width [17].

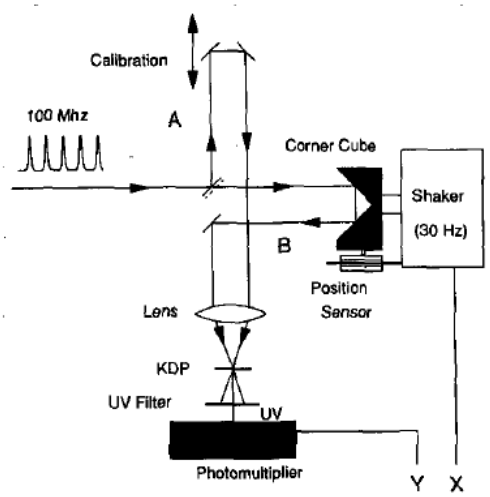

Figure 1. Experimental set-up of the classical second-order autocorrelator.

Figure (8): Autocorrelator schematic [17]

- **Bandwidth and Wavelength:** ***Agilent 86140 series Optical Spectrum Analyzer***

The bandwidth and wavelength analysis were performed on an *Agilent 86140 series Optical Spectrum Analyzer (OSA)*. The OSA provides significant advantages that are vital for the PSL laser characterization. Its visual features include peak search, and auto align. These are useful in quickly refining a sample onto the screen and centering the sample at its peak wavelength. Measurements features include wavelength, amplitude, bandwidth, and trace [18].

- **Power:** ***Optical Power Meter System PM100***

This device inputs the wavelength of the light to output the power to a $\pm 1\%$ accuracy [19]. In our case the wavelength inputted was 1054 nm. It is by this method that we first noticed the drift in power with the modulator bias by creating a program to measure the power over specified amount of time. This program is noted in Appendix A.

- **Jitter measurement and Repetition Rate:** ***Phase Comparator***

A major issue arises when verifying the repetition rate by triggering off a 1.3 GHz reference signal on an oscilloscope. The problem results from the phase fluctuations or *jitter* of the pulse over space and time. Since there is a random jitter with every pulse, measuring the repetition rate

would be random and could change drastically over a long period. The problem is that it would be impossible to indicate how accurate the results are, even if they are averaged over a long duration. However, rather than testing the repetition rate itself, we could test the phase. It has already been determined that if the laser is mode-locked, then the repetition rate is locked to the modulator, the modulator is locked to the frequency, and the frequency is locked to the cavity with the PZT. Therefore the repetition rate can be inferred by comparing the 1.3 GHz signal to a reference 1.3 GHz. If the signal never goes out of phase with the reference it is assured that the signal has the same repetition rate.

With this rationale, it is more reasonable to observe the jitter overtime than the repetition rate. If the laser stays in phase with the reference 1.3 GHz, we can assume that the repetition rate is its proposed 1.3 GHz. The method of preference to measure the jitter is Wilbert S. Rossi *Phase Comparator*. Rossi was a previous A0 intern who worked on developing the phase comparator referred to, to monitor a laser's jitter with respect to the 1.3 GHz.

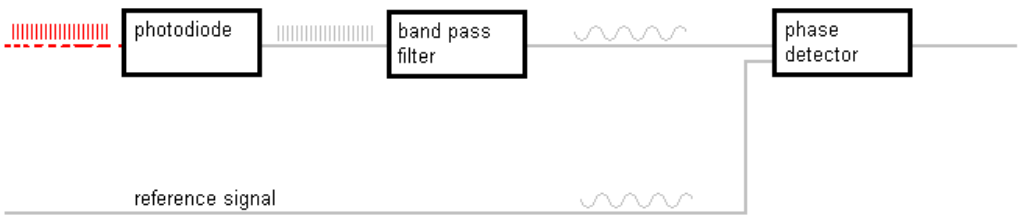

Figure (9): Phase comparator schematic [20].

- **Analysis**

As briefly stated in the introduction, the photons must be directed to the photocathode within the RF-gun using optical media. This media primarily includes lenses and mirrors. For analysis the beam is approximated as a Gaussian. A Gaussian beam has a minimum beam spot (cross sectional area) called its waist, and then it divergences quickly, therefore it is important to keep the beam collimated. The special property a Gaussian beam exhibits when crossing through a lens is total mirroring. The waist is reflected the same distance away from the lens as it originally was from the first waist. This allows for the simple adjustment of beam through the beam pipe, because a component of the optical path, like a mirror, can change the location of a beam waist and the same adjustment will be mirrored on the other side of the lens. This is why is it important to find the location of an initial beam waist, so the location of a secondary waist on the other side of the lens can be predicted.

  - **Beam Spot Analysis:**

This location can be assumed z=0. A form of analysis can then be performed on a laser to find its cross sectional or *beam spot* size at a location z. The beam spot size is the *field amplitude* of the ray. It is measured from the direction of travel z to the perpendicular maximum (typically the x axis) and is reflected in –x. This is defined as $\omega(z)$, and ω_0 is referred to as the *waist* or the minimum beam spot size. For a Gaussian beam, at ω_0 the radius of curvature R is infinite. This property can be used for beam spot calculation with the ABCD law.

- **Using the ABCD Law to find the Beam spot size along z:**

The ABCD law is used to determine the beam spot size along the z axis for a homogenous Gaussian beam. This can be categorized into two cases: with a lens and without a lens. The *Lens Waveguide* characterizes different ray matrices for optical elements and media [10]. The two cases that were necessary for this research were the straight section ray and the thin lens with focal length *f*.

$$\begin{bmatrix} 1 & d \\ 0 & 1 \end{bmatrix}$$ Equation [9]: Straight Section with length $d = z_2 - z_1$ [10]

$$\begin{bmatrix} 1 & 0 \\ -\frac{1}{f} & 1 \end{bmatrix}$$ Equation [10]: Thin lens: Focal length f [10]

If the ray travels through only free space then only the straight section is used, but if the ray travels through free space, hits a lens, then goes back to free space (which is the common case), the matrix is defined by the straight section times the thin lens times the straight section again.

$$\begin{vmatrix} r_{i+1} \\ r'_{i+1} \end{vmatrix} = \begin{bmatrix} 1 & d \\ 0 & 1 \end{bmatrix} \begin{bmatrix} 1 & 0 \\ -\frac{1}{f} & 1 \end{bmatrix} \begin{bmatrix} 1 & d \\ 0 & 1 \end{bmatrix} \begin{vmatrix} r_i \\ r'_i \end{vmatrix}$$ Equation [11]

Where r_i is the input ray and r_{i+1} is the ray out of the lens.

In the ABCD law, the constants A through D are defined by the expanded matrix above:

$$A = 1 - \frac{d}{f}$$ Equation [12a]

$$B = d\left(2 - \frac{d}{f}\right)$$ Equation [12b]

$$C = -\frac{1}{f}$$ Equation [12c]

$$D = 1 - \frac{d}{f}$$ Equation [12d]

These components are used to define a new parameter q, which can be expressed in relation to $\omega(z)$ (beam spot size) to $R(z)$ (the radius of curvature).

$$\frac{1}{q(z)} = \frac{1}{R(z)} - i\frac{\lambda}{\pi n \omega(z)^2} \qquad \text{Equation [13]}$$

It can also be expressed in term of its components:

$$q_2 = \frac{Aq_1+B}{Cq_1+D} \qquad \text{Equation [14]}$$

Here the real part can be used to find the radius of curvature and the imaginary part defines the beam spot size. Therefore, if given the distance from the waist (assuming the waist is at $z = 0$), the wavelength λ, the index of refraction n, and the focal length f, the ω and R at any z can be calculated where $d = z$. A program of this type is available in the Appendix B. Issues with this program arise when the beam spot spacing is very small and the changes in the Gaussian profile are insignificant.

This exact result can also be found if the ray does not cross the lens. This method uses a different set of equations as defined below:

$$\omega^2(z) = \omega_0^2\left(1 + \frac{z^2}{z_0^2}\right) \qquad \text{Equation [15a]}$$

$$R = z\left(1 + \frac{z_0^2}{z^2}\right) \qquad \text{Equation [15b]}$$

$$z_0 = \frac{\pi\omega_0^2 n}{\lambda} \qquad \text{Equation [15c]}$$

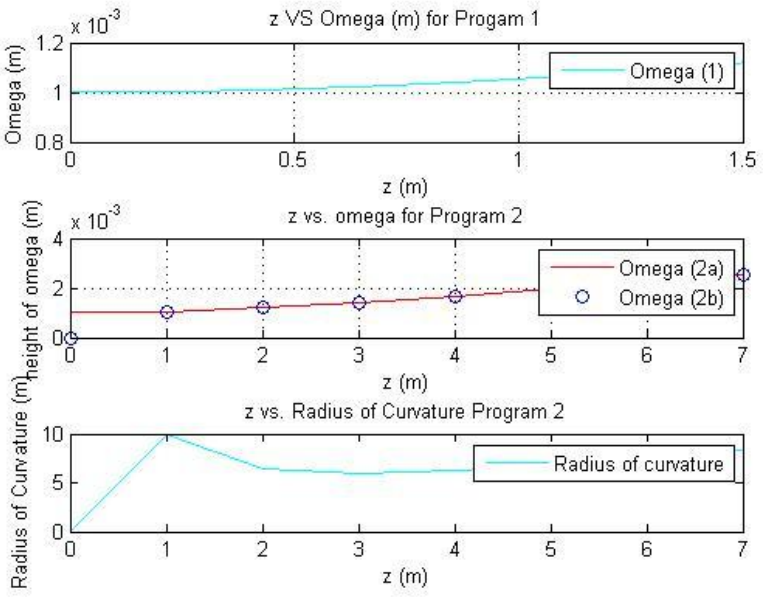

Figure (10): Plot with $\lambda = 1054\ nm, n = 1, f = 20\ m, L = 20\ m$. L is the distance of the thin lens from the origin. The second plot is produced from program 2. The circles are the results of equations [15], and the solid line plots the

beam spot using equation [13]. The first plot uses the beam spot information at ω_1=5 m, ω_2=7 m, with a distance of 2 m between them. It provides the same information as the 2nd program, but from reversed information. This method is defined in the next section.

- **Finding the location of the waist**
  - **Approximation**

There is also a way to perform the reverse of the beam analysis without a lens. This means to find the location of the waist given two beam spot sizes and the distance between the two. The first step gives an approximation, which is accurate for spot sizes much greater than the Rayleigh length distance.

This technique first requires finding the *angular spread* or *divergence* of the beam. This can be approximated by the slope between the two beam spot size heights using the distance between them. This is used to approximate ω_0 as defined below:

$$\theta_{beam} = \tan^{-1}\left(\frac{\lambda}{\pi\omega_0 n}\right) \qquad \text{Equation [16]}$$

The distance to the waist can be found from the relations defined previously (equation [15a]) and the Rayleigh length z_0 (equation [15c]). The waist is the distance along z of the $\omega(z)$ value producing the smaller z value.

- **Accurate Approach**

The next step uses the approximation as a searching point for the real ω_0. The two beam spot sizes can be expressed in terms of ω_0 from equation [15a]:

$$\omega_1^2 - \omega_0^2 = \frac{\lambda^2 z_1^2}{\pi\omega_0^2} \qquad \text{Equation [17a]}$$

$$\omega_2^2 - \omega_0^2 = \frac{\lambda^2 z_2^2}{\pi\omega_0^2} \qquad \text{Equation [17b]}$$

These equations can be arranged, so that z_1 and z_2 are no longer needed.

$$\sqrt{\omega_2^2 - \omega_0^2} - \sqrt{\omega_1^2 - \omega_0^2} = \sqrt{\frac{\lambda^2 z_2^2}{\pi\omega_0^2}} - \sqrt{\frac{\lambda^2 z_1^2}{\pi\omega_0^2}} = \sqrt{\frac{\lambda^2}{\pi\omega_0^2}}(z_2 - z_1) \qquad \text{Equation [18]}$$

With this equation it is possible to solve for ω_0. A method that can be utilized to solve for the equation is the function *fminsearch* in Matlab. The distance to the closest beam spot can be found using equation [15a] after updating the z_0 value with the new ω_0.

- **Computer Interface PM100: Serial Programming**

It was necessary to develop a Matlab program to process the data returned by the PM100 power meter. After the method was established to connect the power meter, a program was written with the assistance a programmer to read out the power measurements of the laser over a specified time period. The PM100 needed to be interfaced over a serial port. The program reads out the power from the PM100 and saves it to a vector *u*. It also records the times each reading is made to vector *time*. It plots these vectors against each other. After the time reaches a specified duration the program stops and displays the final time. This process is shown below, and the code is available in Appendix A.

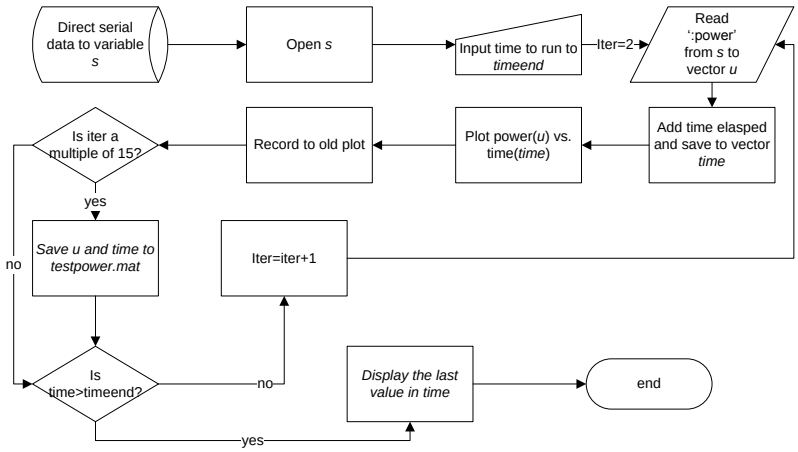

Figure (11): Power programming flowchart

- **Results**
  - **Laser Characterization**

An RF spectrum of the signal was taken with the OSA as shown in figures (12a),(12b), and (12c). Figure (12a) displayed the spectrum zoomed out, so details are not visible, but it is clear that the peak of the spectrum is located at approximately 1.3 GHz. Figure (12b) shows the spectrum at a modulator bias voltage of about -3 V. The modulator bias voltage produced sidebands in the spectrum. Figure (12c) displayed the optical spectrum at a modulator bias voltage of 1.51 V. At this voltage, the sideband are not visible, however the power of the signal is much lower than what is proposed. The spectrum available in the laser manual depicts a power of -10 dBm, but the trace that was taken is at -50 dBm.

To characterize the power a power meter was used. The power was taking over a 24 hour period and a constant modulator bias voltage. The fiber output terminal that remains unamplified exhibited a downward trend. This trend was fit to a linear line with a slope of -1.11×10^{-9} mW/hr. The mean power of the sample was 0.79 mW, and the standard deviation was 0.028 mW. Similarly, the power was monitored over a 24 hour period via the amplified port. This port was amplified using a 404 mA amplifier current. This data was also fit to a linear line with a slope -1.11 mW/hr. The mean of this data was 63.7 mW and the standard deviation was 7.6645 mW.

Rather than keeping the modulator bias static, the power was scanned over the span of the modulator bias voltage. The span ranges from -4.35 V to 4.50 V. This was done over several periods of runtime after PSL start up. The colored curves correspond to a different runtime, from 24 hours to 4 days. The detail to note about these curves is that the maximum and minimum powers shift quite randomly. For example, during one trial the minima will occur at 0 V, the next day it was occur and -1.5 V, and the next is will occurs at 3 V. The only thing to be concluded from this knowledge is that the modulator bias drifts randomly over time. This could be attributed to the DC drift phenomena mentioned in the Electro-optic Modulator & Modulator Bias control section.

- **Initialization**

First time setup of the system was more or less simple, but issues occurred with the initial run. Temperature stabilization at 38℃ took more than 2 hours. In addition, problems were noted when the power was first monitored. Maximum power (according to the manual) was unattainable with the initial setup parameters. These parameters are outlined in the table below:

Name	Range	Initial Optimum Value	Note
RF Drive Frequency		1.30016 GHz	
RF Drive Power		5 dBm	Occasionally varying RF power by 0±2 dB may help achieve low noise
Laser Temperature		38.0 °C	
Modulator Bias	-4.35 ~ 4.50 V	-2.50 V	Modulator bias voltage influences stability and pulse width. Optimal bias voltage usually drifts quickly during initial operation.
Phase Shifter	0 ~ 16.12 V	9.68	The phase shifter voltage influences the stability of the laser. The optimal phase shifter value strongly depends on the RF drive frequency, pump current and modulator bias.
Seed Laser Pump Current	0 ~ 379 mA	300 mA	Seed laser pump current influences output power, output pulse width, and output stability.
Amplifier Pump Current	0 ~ 405 mA	405 mA	Amplifier pump current influences output power

Table [1]: Initial setup parameters [7]

Our first time setup parameters were: 1.30015 GHz, 1.48 dBm, 38℃, -2.50 V, 9.68, 300 mA, and 404 mA, which are all within the allowable range for variation. The rest of the setups are available in the table below.

Test Parameters	**2st Time (06/22/2010)**	**3nd Time (07/14/2010)**	**4rd Time (0726/2010) Power outage**
RF Drive Frequency	1.30015 GHz	1.3000009389 GHz	N/a
RF Drive Power	1.48 dBm	3.49 dBm	N/a
Laser Temperature	38 ℃ after about 3 hours	37.9 ℃ after about 3.5 hours	38.4℃ to 38 ℃ in 2 hours

Modulator Bias	-2.50 V	-2.50 V	-2.50 V
Phase Shifter	9.69	9.68	9.68
Seed Pump Current	300 mA	300 mA	300 mA
Amplifier Pump Current	404 mA	404 mA	404 mA

Table [2]: Our parameters at each setup

First we informally investigated the signal produced on an oscilloscope. The signal observed was indecipherable and looked more like noise than a signal. Subsequently, the signal power was tested with a power meter. It was noted that the power drifts significantly with time, so a power measurement was conducted over a longer duration. The results of these tests are available in figures [12a],[12b], and [12c].

- Important Occurrences

There are some important things to note when starting up the laser. After setting the initial parameters the temperature stabilizes about 3-5 hours after startup rather than 30 minutes as denoted in the manual. For optimal stability, as with most laser system, it is preferable that the laser remain on for at least 1 day, but 2-3 is preferable. Output A produces a more stable power output over a long period of time; however the effects of the amplifier are still unknown. Some of the plots below will display the stability of the laser over certain time intervals.

After some initial investigation it was noted that the drift in the power relates to the modulator bias. We were able to determine that over a long period of time (about 2-3 days) that the laser runs significantly more steadily. The power does not drift as significantly, but it does still drift. This could be related to the DC drift phenomena, which was discussed in the Electro-optic Modulator & Modulator Bias control section however, direct relation is unknown. Plots of the power vs. modulator bias are available in figure [15], and [16].

Since we could not produce a decipherable oscilloscope trace we needed to also check how well the laser was locking to 1.3 GHz. We were able to do this with the optical spectrum analyzer. Surprisingly, we noticed a relationship between the modulator bias and the optical spectrum. At certain modulator bias voltages (around -3 V) sidebands would appear in the spectrum. The sideband would disappear by adjusting the modulator bias to 1.51 V corresponding to a power of 52.64 mW. The OSA also registered a power of -50 dBm, which is significantly lower than the power noted in the manual at -10 dBm. If we could not produce a clean spectrum it would not be necessary to run a jitter measurement, because the phase depends very strongly on how well the laser locks to 1.3 GHz.

Date	**Occurrence**	**Description/Reading**	**Solution**
06/22/2010	Temperature stabilization	Took about 3 hours to stabilize	Accepted as normal
	Output power vs. Modulator Bias voltage	Output power changes with modulator bias	Plot
	Output power vs. Amplifier Pump current	The power is lower than the plot described in the manual	Plot and ask Calmar Lasers
06/15/2010	Output power B	Output power B drifts a lot	Plot

06/16/2010	Mod. Bias for Max. power	Shifts with time	Plot over time and fit
07/20/2010	Mod. Bias for Min. power	Shifts with time	Plot over time and fit
07/21/2010	Sidebands in optical spectrum	Modulator Bias changes optical spectrum	Plot

Table [3]: Important first time occurrence dates and descriptions

- Plots and Data

Wavelength & Bandwidth

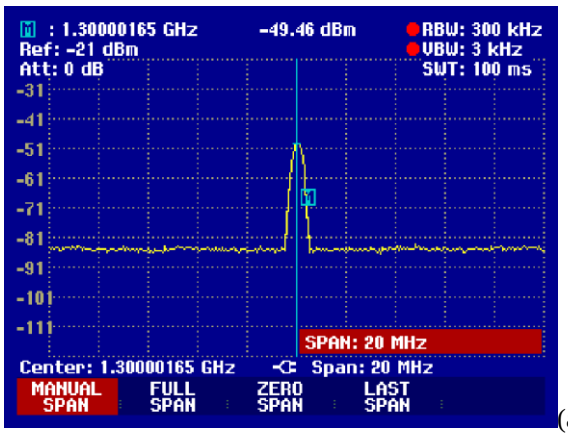

(a)

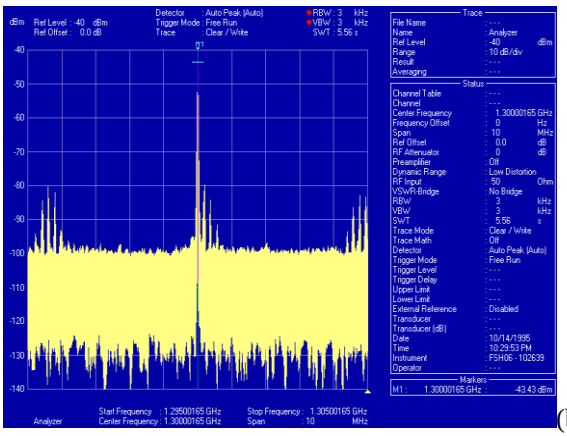
(b)

Figure (12): *OSA* traces of RF spectrum. Plot (a) displays a low video bandwidth for a zoomed out effect. Plot (b) has sidebands from modulator bias adjustments at ~-3.00 V. Plot (c) shows a power much lower than the power denoted in the manual (-10 dBm), but sibebands are depleted with modulator bias adjustments (1.51 V).

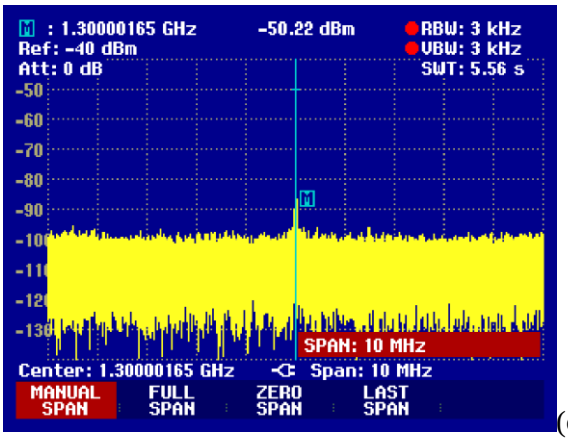

(c)

Power

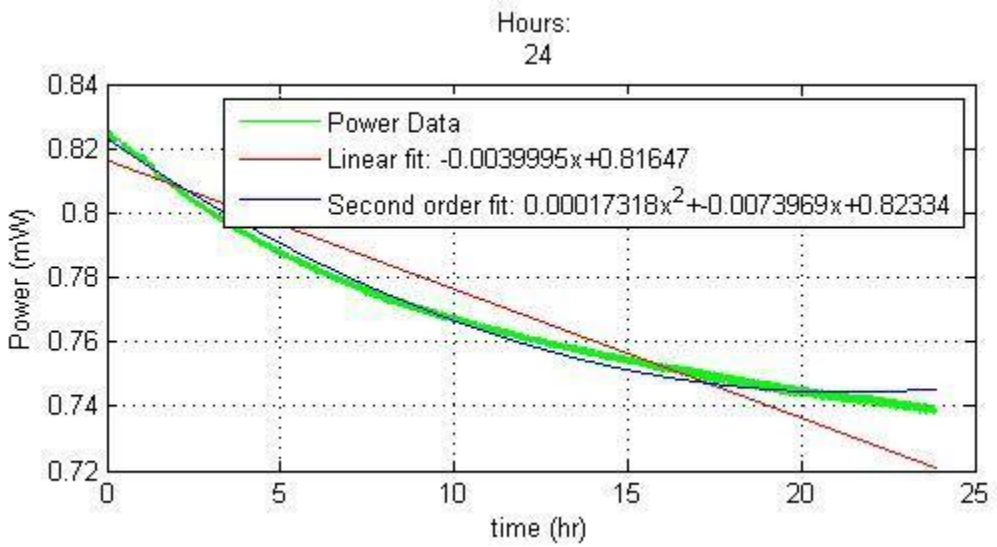

Figure (13a): Matlab plot from port B over 24 hours after 1 week of running. Mean power was 0.79 mW and standard deviation was 0.028252 mW. The slope of the curve if approximated by a linear line is -1.1110e-009 W/s which also corresponds to a 10.2809% drop from its initial value in 1 day.

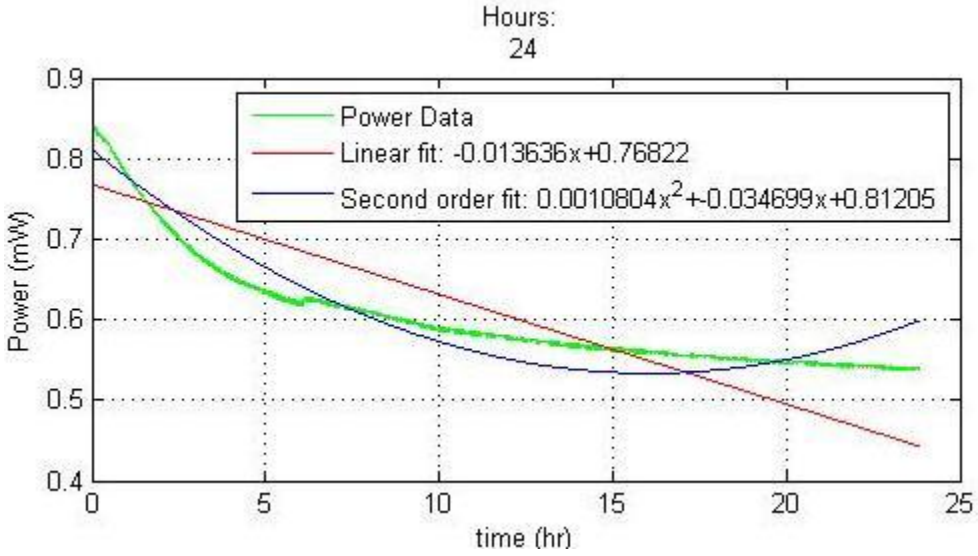

Figure (8b): This data was taken after 30 hours of running from output B. This preliminary data was taken over a 24 hour period. Mean power was 0.6820 mW and the power drop in a day was 35.9913%. The slope of the curve if approximated by a linear line is -0.013636×10^{-9} mW/hr.

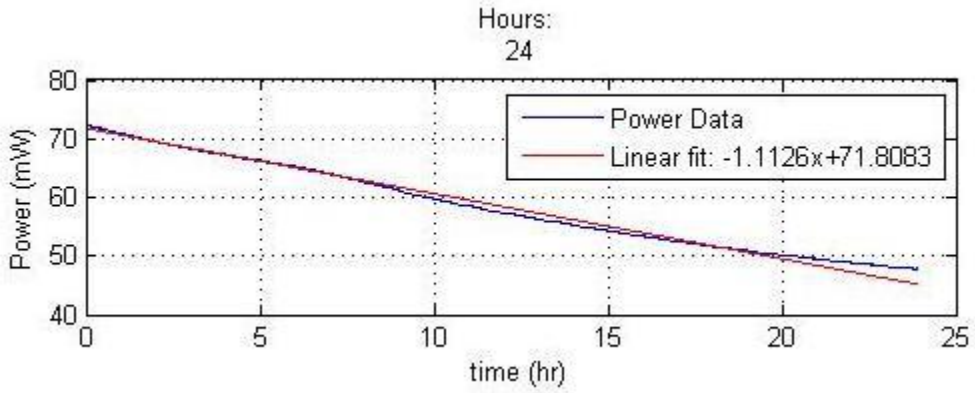

Figure (9): Matlab plot from port A after about a 56 hour runtime. This data was taken over about a 24 hour period. Mean power was 63.7559 mW and the power drop is a day was 33.8583%. The slope of the curve if approximated by a linear line is -1.1126 mW/hr.

Modulator Bias Over Time and Power

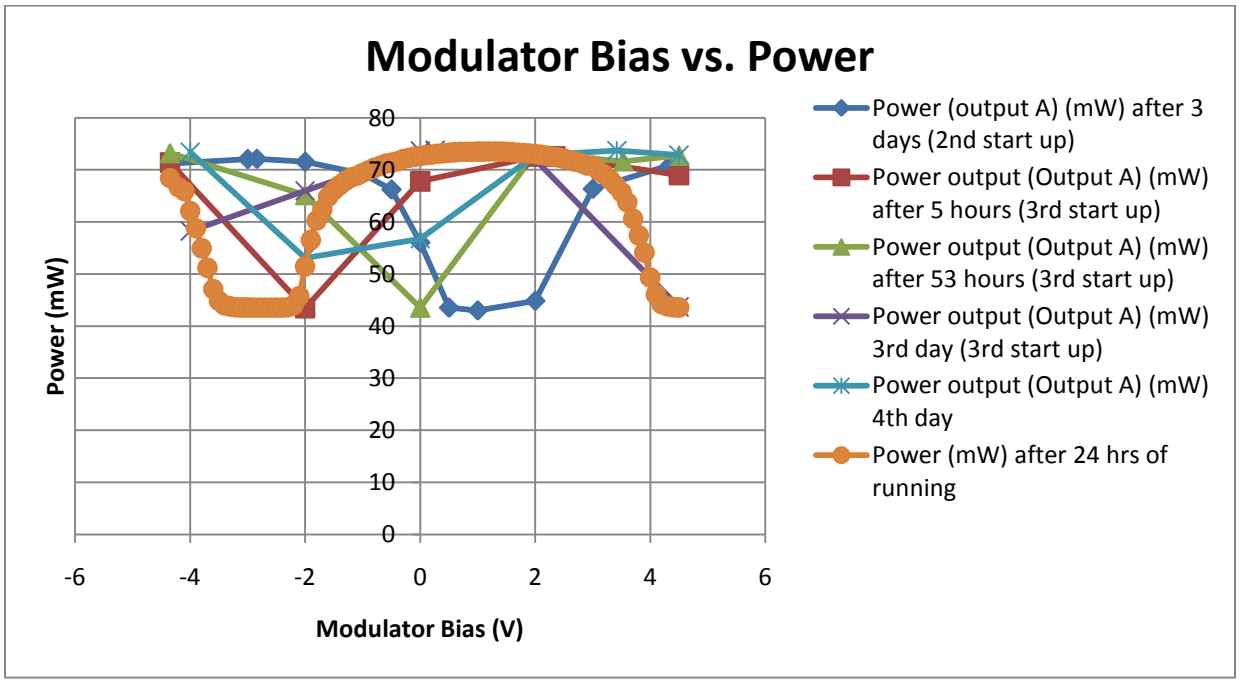

Figure (15): It can be easily seen that the maximum (and minimum) modulator bias shift with time, however the overall shape of the curve remains the same.

Detailed Modulator Bias vs. Power Curve

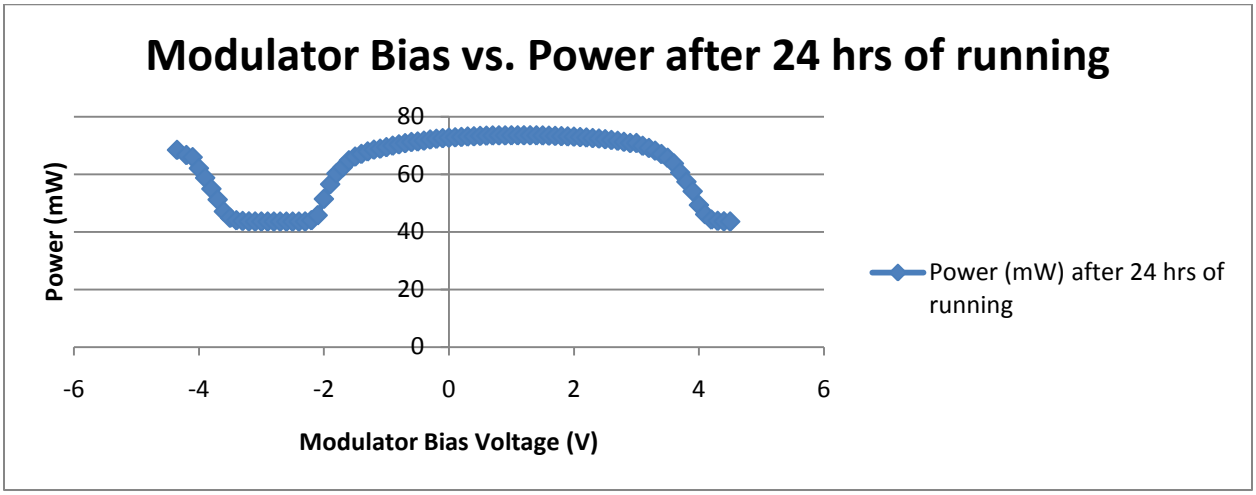

Figure (16): The curve was taken after about 24 hours of run time.

Conclusion:

In conclusion, the PSL analysis will need to be done more in-depth. From what is known the laser can lock stability to 1.3 GHz, as depicted by the OSA trace without sidebands. This occurred at a modulator bias of 1.51 V. But, it is also important to note that the sidebands occur at another modulator bias point (-3 V). This expresses the direct relation between the PSL's mode-locking ability, and its spectra.

In addition, the power is significantly below expected. From startup it was not possible to obtain the optimal power, with the startup parameters. Upon testing the power against a constant modulator bias voltage, the output power displayed a downward trend over time. During some tests the decrease was not significant (refer to figure (8b)), but the downward is always evident. It is suspected that the reason for the downward trend is because the modulator bias for the maximum power shifts with time as depicted in figure (15).

Perhaps the "s" shape of the power curve (refer to figure (16)), while scanning the modulator bias, will not affect the performance of the PSL, but the power drift undoubtedly will. It is necessary that the modulator bias is monitored and remotely programmed to optimize the PSL for mode-locking to 1.3 GHz, and for maximum power. However, as shown in figure (12c) and (12c), these two modulator bias points are not necessarily the same. The modulator bias point for optimal power is not the same as the modulator bias for a clean optical spectrum. This will also have to be looked into further to find an equilibrium point between the two.

Future Work:

In the near future more research will have to be performed on this laser before it can be implemented to replace the A0 laser in NML. Some important projects would include the setup

of the autocorrelator for pulse width characterization. This is the most accurate method to measure the pulse lengths of ultra-short pulses.

In addition, jitter measurements would have to be conducted with respect to 1.3 GHz. All tests could be compared and contrasted with the current laser. If the PSL provides comparable measurements, then it is very likely it will replace the seed laser in A0 for NML. The most important tests would include jitter, pulse width, and wavelength. It is also very important to determine the point for optimal spectra and power.

The "deal-breaking" factor designating whether the PSL will replace the A0 laser falls upon power stability. At present, though simple, this is the biggest flaw the laser exhibits. Since the photon pulses produced by the seed laser are directly mirrored in the photoelectron bunches that are produced by the photocathode, if these photons are not identical, then the electrons will have the same incongruence. Therefore, it is very important to create a feedback program to be interfaced with the modulator bias voltage. This program will remotely adjust the modulator bias voltage for the its best mode-locking performance and maximum power. If this is not possible, then other measures will have to be implemented to compensate for the modulator bias drift.

Acknowledgments:

I would like to express by deepest thanks to my supervisor Jamie Santucci and my co-supervisor Jinhao Ruan for continually helping and explaining every aspect of my research and testing including the programming. I would also like to express gratitude to the A0 staff, including Amber Johnson, Tim Maxwell, Alex Lumpkin, Randy Thurman-Keup, Elvin Harms, Helen Edwards, Yin-e Sun, Philippe Piot, and Vic Scarpine for helping me through my presentation(s). I would also like to thank Stewart Mitchell and A0 drafting for all the technical support. A deep appreciation goes to Dianne Engram, Linda Diepholz, Jamieson Olsen, James Davenport, Dave Peterson (my SIST mentor) and LaMargo Gill for this internship opportunity and support along the way. And lastly but not least, a special thanks goes out to Maurice Ball, the co-op crew, the A0 interns of summer 2010, and all the SIST and GEM interns especially my housemates for such a great summer.

Appendix:

- Appendix A: Power Monitor Programming

Serial Interface

```
%%
s=serial('COM19','BaudRate',115200,'Databits',8); %might need to change COM20
set(s,'FlowControl','hardware')
set(s,'Terminator',{'CR/LF','LF'})
fopen(s)
%%
```

```
timeend=60*60*24; %set the duration in seconds
iter=2;
tic;
time=[];
u=[];
while (1)
fprintf(s,':POWER?')
tmp=fread(s,14);
pause(1);
y=char(tmp');
u(end+1)=str2num(y);
time(end+1)=toc;
plot(time,u,'*'),xlabel('time (s)'),ylabel('power (W)'),title('Time VS.
Power');
hold on
if(mod(iter,15)==0)
    save('testpower.mat','time','u')
end
if time(end)>=timeend, break, end
iter=iter+1;
end
disp('The time of the whole cycle is: '),time(end)
%s % to check if the device is communicating
```

Error

```
%error curve fitting
load('testpower_12.mat'); %load the mat file
time_final_hours=ceil(time(end)/(60*60))
least=polyfit(time,u,1); %do a linear last squares fit
f=@(x) least(1)*x+least(2); %creates best fit line
subplot(2,1,1), plot(time,f(time),'r',time,u), xlabel('time
(s)'),ylabel('Power (W)'),title({'Hours: ';time_final_hours}); %change to mW
grid on
text(time(end)*.89/2,max(u),'Slope: ');
text(time(end)/2,max(u),num2str(least(1)));
text(time(end)*1.13/2,max(u),'(W/s)');
legend('Least squares line','Data');
RMS=sqrt(mean(u.^2))
mean_value=mean(u)
standard_deviation=std(u)
slope=least(1)
percent_drop_in_1_day=slope*60*60*24*100/u(1)
for i=1:length(u)
    SNR=f(time(i))/u(i); %signal to noise ratio
    SNRdb=10*log10(SNR);
end
subplot(2,1,2), loglog(time,SNRdb,'m'), xlabel('time (s)'), ylabel('SNR
(db)'),title('Signal-to-Noise Ratio');
```

- Appendix B: Waist Programming

```
function y=gaussianplot(lambda, n_i, t, f, L)
```

```
format long eng
%6 inputs
%1) lambda- wavelength (m)
%2) n_i- index of refraction
%3) t- number of spot sizes to be measures
%4) f- focal length (m)
%5) L- location of lens (m)
disp('input 1 for omega_0 for z far from the waist, input 2 for beam spot
size at z: ')
choose=input('1/2 ?: ');
if choose==1
    %LOCATION OF WAIST for z
    %known: omega1, omega2, d-distance between them
    mycolor=['c','m','y','k','r','g','b','w','x','*','o']; %matrix of 11
colors
    beamspot=input('input column vector [d(i), omega(z(1)), omega(z(2))]: ');
    slope=abs(beamspot(2)-beamspot(3))/beamspot(1);
    omega_0=lambda/(pi()*n_i*tan(slope)); %minimum waist size
    %compare angles:
    theta_beam=lambda/(pi()*omega_0*n_i); %based on p.113
    atan(slope); %only true if the beam spot sizes are far from the waist
    z_0=(pi()*omega_0^2*n_i)/lambda
    d_along_z=@(o,omega_0) sqrt(o^2/omega_0^2-1)*(pi*omega_0^2*n_i/lambda);
    if beamspot(2)>beamspot(3)
    %z(1)=d_along_z(beamspot(2),omega_0,z_0)
    z(2)=beamspot(2)/tan(slope)
    z(1)=z(2)-beamspot(1)
    else
    %z(1)=d_along_z(beamspot(3),omega_0,z_0)
    z(2)=beamspot(3)/tan(slope)
    z(1)=z(2)-beamspot(1)
    end
    ZR=(pi()*omega_0^2)/lambda; %rayleigh length: length of the waist from
the origin
    if real(z(2))>real(z(1)) && real(z(1))~=0
        z_waist=z(1);
    elseif real(z(1))>real(z(2)) && real(z(2))~=0
        z_waist=z(2);
    elseif real(z(1))==0
        z_waist=z(2);
    elseif real(z(2))==0
        z_waist=z(1);
    elseif z(1)==z(2)
        error('same spot size');
    end
    hold on
    disp('z_waist, omega_0 approximation: ')
    [z_waist omega_0]
    %plot omega_0 for all z using the approximation from the first one
     omega1=beamspot(2);
     omega2=beamspot(3);
     d=beamspot(1);
     fun2= @(x)abs((pi*x*(sqrt(omega1^2-x^2)-sqrt(omega2^2-x^2))/lambda-d));
     %function fminsearch
```

```
     xr =
abs(fminsearch(fun2,omega_0,optimset('display','iter','TolX',10,'TolFun',1e-
30,'MaxIter',1e30,'MaxFunEvals',1e30)));
     omega_0_new=xr
     z_0_new=(pi*omega_0_new^2*n_i)/lambda
     zn(1)=d_along_z(beamspot(2),omega_0_new)
     zn(2)=d_along_z(beamspot(3),omega_0_new)
    if real(zn(2))>real(zn(1)) && real(zn(1))~=0
        z_waist_new=zn(1);
    elseif real(zn(1))>real(zn(2)) && real(zn(2))~=0
        z_waist_new=zn(2);
    elseif real(zn(1))==0
        z_waist_new=zn(2);
    elseif real(zn(2))==0
        z_waist_new=zn(1);
    elseif zn(1)==zn(2)
        error('same spot size');
    end
    w=@(z) sqrt(omega_0_new^2*(1+z.^2/z_0_new^2)); %equation for new omega(z)
     U=0:0.01:1.5;
     subplot(3,1,1), plot(U,w(U),mycolor(1)), ylabel('Omega (m)'), xlabel('z
(m)'), title('z VS Omega (m) for Progam 1');
     legend('Omega (1)')
     grid on
     disp('z_waist, omega_0 accurate: ')
     y=[z_waist_new omega_0_new];
elseif choose==2
    %BEAM SPOT SIZE
    omega_0=input('omega_0: (m)'); %omega_0- minimum waist (m)
    %---at the waist---
disp('You are going to take:'), disp(t-1), disp('measurements. BEGIN:'),

m=2; %need atleast one measurment less than the distance to the lens
e=1;
z=zeros(1,t); %z matrix
q=zeros(1,t); %q vector
R=zeros(1,t); %radius of curvature vector
omega=zeros(1,t); %beam spot size matrix
omega_r=zeros(1,t);
omega(1)=omega_0;
z_L=zeros(1,t);
omega_L=zeros(1,t);
v=zeros(2,2*t); %initial matrix to hold a,b,c,d where a=v(1,1), b=v(2,1).
c=v(2,1), d=v(2,2)
q_z=(-1i*lambda/(pi()*n_i*omega_0^2))^-1; %spot size at the waist
q(1)=q_z; %first is q(0) or waist hieght
while (1)
z(m)=input('input the location of the spot size you want calculated: (m) ');
if z(m)>=L-1 && z(m)<=L+1
        disp('MUST INPUT A MEASUREMENT AT THE LENS FOR ACCURATE RESULTS!
at:'), disp(L)
end
%ABCD matrix for each measurement z(c)
A_i=[1 z(1); 0 1]; %initial matrix A_1
if z(m)< L || z(m)>L
    A=[1 (z(m)-z(m-1));0 1]; %straight section p.101 table 6.1 (1)
```

```
    v(1:2,e:e+1)=A;
else
    A_0=[1 L-z(m-1);0 1]; %straight
    B=[1 0; (-1/f) 1]; %thin lens p.101 table 6.1 (2)
    A_B=B*A_0; %straight section & thin lens
    v(1:2,e:e+1)=A_B;
end
%turning ABCD into scalars
    g=1:length(v);
    a(m-1)=v(1,g(e));
    b(m-1)=v(1,g(e)+1);
    c(m-1)=v(2,g(e));
    d(m-1)=v(2,g(e)+1); %weird script wont be inputted in order
    %assign a new q
q(m)=(a(m-1)*q(m-1)+b(m-1))/(c(m-1)*q(m-1)+d(m-1)); %value of q for that z
%---thin lens: for the firsts section only use straight section, and for
%the second part use the straight section*lens*straight section*******
%---equation 6.6-14a p.112
    omega(m)=(sqrt(-lambda/(imag(1/q(m))*pi()*n_i)));    %spot size
   %p. 111
    z_0=(pi()*omega_0^2*n_i)/lambda;
    omega_r(m)=sqrt((omega_0^2)*(1+(z(m)^2/z_0^2)));
    R(m)=1/real(1/q(m)); %radius of curvature
    i=0;
    if z>=L %when z is passed the lens
    z_L(i)=z(m);
    omega_L(i)=omega(m);
    i=i+1;
    end
[z_L;omega_L];
subplot(3,1,2), plot(z,omega, 'r',z,omega_r,'o'),  xlabel('z (m)'),
ylabel('height of omega (m)'), title('z vs. omega for Program 2');
legend('Omega (2a)','Omega (2b)')
grid on
subplot(3,1,3), plot(z,R, 'c'), xlabel('z (m)'), ylabel('Radius of Curvature
(m)'), title('z vs. Radius of Curvature Program 2')
legend('Radius of curvature')
m=m+1; %iterate the z measurements
e=e+2; %iterate the abcd matrix

if m>t||e>=length(v), break, end
end
disp('***Matrix of ROW 1-Z; ROW 2-omega;ROW 3-R; Row 4-q;***'), y=[z; omega;
omega_r; R];
ZR=(pi()*omega_0^2)/lambda;
else
    %ERROR MESSAGE
    error('You must choose 1 or 2.')
end
```

- Appendix C: Images and Pictures
    - PSL

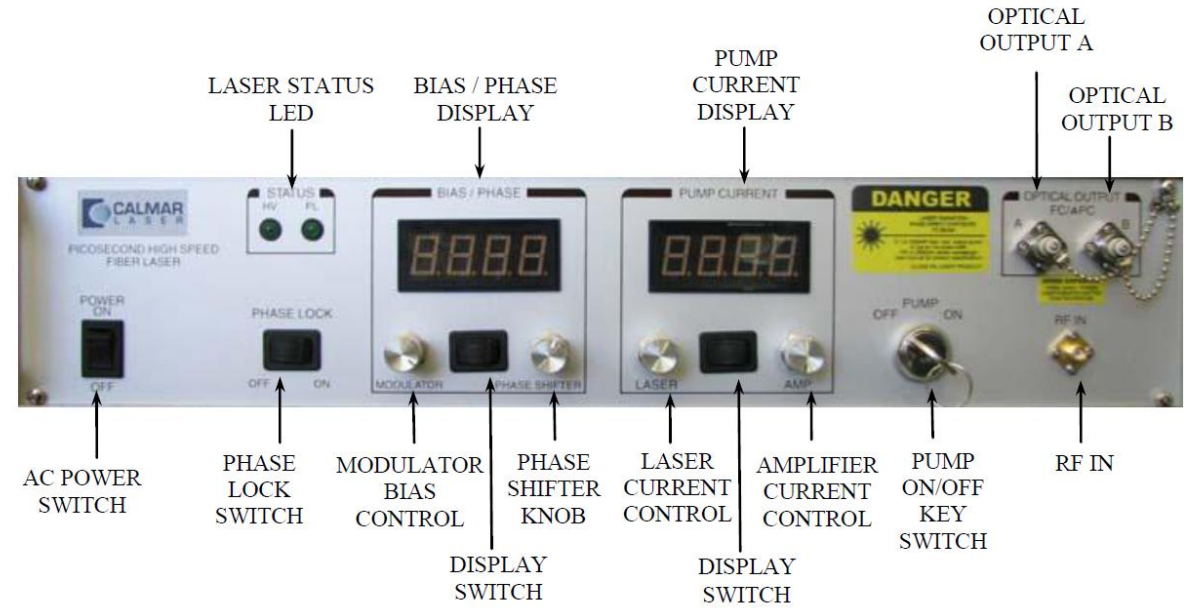

Figure (17): Front panel [7]

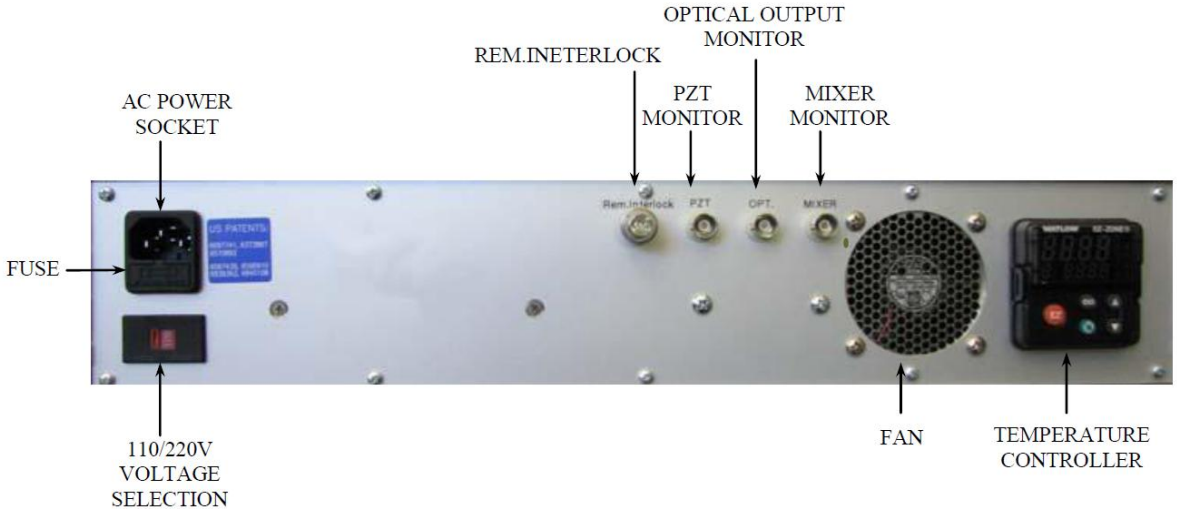

Figure (18): Rear panel [7]

References:

[1] Office of High Energy Physics, Office of Science, U.S. Department of Energy, "Exploring the Quantum Universe," June 2010, http://www.science.doe.gov/hep/index.shtml.

[2] U.S. Department of Energy, "National Labs," July 2010, http://www.energy.gov/sciencetech/nationallabs.htm.

[3] Fermilab, "Fermilab Facts," January 2010, http://www.fnal.gov/pub/presspass/factsheets/pdfs/Fermilab_Overview_2010.pdf.

[4] A0 Photoinjector and SCRF Facilities, Fermi National Accelerator Laboratory, "A0 Photoinjector and SCRF Facilities," June 2010, http://www-a0.fnal.gov/.

[5] DESY, "Getting There," July 2010, http://www.desy.de/about_desy/getting_there/index_eng.html.

[6] Antonine Education, "em_spectrum.jpg," July 2010, http://www.antonine-education.co.uk/physics_gcse/Unit_1/Topic_5/em_spectrum.jpg.

[7] Calmar Lasers, Inc, "Picosecond Pulsed Fiber Laser Instruction Manual," Manual No.: Man-880690.

[8] Winter, Axel, "*Fiber Laser Master Oscillators for Optical Synchronization systems."* PhD diss., University of Hamburg, Germany, 2008.

[9] Porta Optica, "Chormatic Diserpsion," July 2010, http://pos.lumii.lv/uploads/prezentacijas/piotr-4.pdf.

[10] Yariv, Amnon. "The Propagation of Optical Beams in Homogenous and Lenslike Media" & "Q-Switching and Mode Locking of Lasers", in *Quantum Optics*, 2nd ed. New York: John Wiley & Sons: 1975, ch. 6, pp. 99-115, ch. 11, pp. 256-262.

[11] Optoelectronics Business Division, Sumitomo Osaka Cement Co., LTD, "Application Note for LN Modulators", July 2002, http://www.lambdaphoto.co.uk/pdfs/SumitomoModulatorApplicationNote.pdf.

[12] University of Cambridge, "Population Inversion," July 2010, http://www.sp.phy.cam.ac.uk/~SiGe/Population%20Inversion.html.

[13] Wikipedia, "Stimulated Emission," July 2010, http://en.wikipedia.org/wiki/Population_inversion#Stimulated_emission.

[14] Encyclopedia of Laser Technology, "Ytterbium-Doped Gain Media," July 2010, http://www.rp-photonics.com/ytterbium_doped_gain_media.html.

[15] Calmar Laser, Inc., "Low Dispersion Amplifier Instruction Manual," Manual No.: Man-880691.

[16] Calmar Laser, Inc., "Electronic Pulse Generator Instruction Manual," Manual No.: Man-880689.

[17] A. Brun, P. Georges, G. Le Saux, and F. Salin, "Single-Shot Characterization of Ultra-short light pulses," J. Phys. D: Appl. Phys. 24, U.K.: January 1991, pp. 1226-1233.

[18] Agilent Technologies, "Agilent 86140B Series Optical Spectrum Analyzer User's Guide," http://cp.literature.agilent.com/litweb/pdf/86140-90068.pdf.

[19] Thorlabs Instrumentation, "Optical Power Meter System," 2006, http://www.thorlabs.com/Thorcat/12200/12271-D02.pdf.

[20] Rossi, R. S., Physics Eng., Turin Polytechnic, "Phase comparator" Accelerator Div., Fermilab, Summer 2009.